

Received June 10, 2020, accepted July 1, 2020, date of publication July 9, 2020, date of current version July 22, 2020.

Digital Object Identifier 10.1109/ACCESS.2020.3008257

Energy-Efficient Biocooperative Video-Aware QoS-Based Multiobjective Cross-Layer Optimization for Wireless Networks

YAKUBU S. BAGUDA , (Senior Member, IEEE)

Information Systems Department, Faculty of Computing and Information Technology, King Abdulaziz University, Rabigh 21911, Saudi Arabia

e-mail: ysoleman1@kau.edu.sa

This work was supported by the Deanship of Scientific Research (DSR), King Abdulaziz University, Saudi Arabia, under Grant DF-802-830-1441.

ABSTRACT Video streaming is becoming increasingly popular due to the emergence of different video applications and services and the exponential growth in demand for multimedia applications. Streaming video over an error-prone network is technically challenging due to unpredictable channel conditions and demands for different types of quality of service (QoS) from various types of applications. The traditional Open System Interconnection (OSI) layered approach is designed for data transfer, and it performs specific operations independent of other layers. This approach may not work efficiently for wireless video streaming applications in which video quality is greatly affected by the network condition, link quality, and ability of the system to adapt to the channel conditions. This paper is primarily aimed at developing an algorithm to enhance video streaming over wireless local area networks using a biocooperative video-aware QoS-based multiobjective cross-layer optimization (MO-CLD) approach. First, the wireless video streaming optimization problem is formulated and modeled. To solve the optimization problem, we proposed a bioinspired optimization algorithm to jointly optimize the source rate and packet rate loss using dual decomposition. The simulation results show that the proposed biocooperative multiobjective optimization scheme using particle swarm optimization (PSO) relatively maintains and enhances the video streaming quality in error-prone transmission environments to ultimately support wireless multimedia applications and services. More importantly, the end-to-end delay and complexity are reduced significantly, which eventually lead to improvements in the scheme efficiency and video quality compared to basic cross-layer optimization (B-CLD).


INDEX TERMS Biocooperative, energy efficient, multiobjective cross-layer optimization, particle swarm optimization, quality of service, wireless network.

I. INTRODUCTION

The demand for multimedia streaming applications and service is increasing exponentially and has dramatically reshaped the telecommunications industry to new dimensions with the development of various video applications. Future wireless communication systems are expected to provide a broad range of multimedia services, including voice, video, and data [1]–[3]. This will have a profound impact on the way individuals communicate and access information. Many applications and devices use wireless media to share

information and to transport data across the network. The advancements in video coding, electronics and networking will lead to the development of new wireless multimedia applications and services [3], which will require more efficient strategies to transport video applications over wireless networks.

Multimedia applications have been used in surveillance, education, entertainment, security, and monitoring. It is extremely important to provide adequate quality of service (QoS) to support these applications, especially in wireless communication media [4]–[6], due to the video application delay constraint [22]. Video applications primarily include video-on-demand, distance learning and training,

The associate editor coordinating the review of this manuscript and approving it for publication was Zihuai Lin .

interactive gaming, remote shopping, video telephony, video conferencing, and remote surveillance. The high demand and need to support different kinds of devices with different QoS, throughput and heterogeneous terminals with a wide range of capabilities and user preferences is very crucial. The ability to access multimedia content requires adaptation of media content based on user interactivity. There is a need to bridge the gap between the media content and techniques used. The possibility of ensuring QoS in wireless multimedia networks depends greatly on the robustness and resilience of the scheme used [10]. Thus, there is need for highly efficient, robust and adaptable strategies to ultimately support video applications and services. Transporting video over wireless networks is challenging and difficult due to the wireless network dynamics and heterogeneity [3], [7], [8], [52], [55].

To ultimately support and transport video data over a wireless network, a more in-depth knowledge, comparative evaluation and development of new strategies are necessary to critically assess the possible trade-offs in multimedia quality, implementation complexity, and power consumption [9]. Hence, more efficient strategies are needed to mitigate the impact of time-varying channels on the transmitted video data. Interestingly, cross-layer design (CLD) has been proposed as a possible solution to adapt to channel conditions and to provide the required QoS needed [11], [25], [46]–[51] for wireless multimedia communications. The need for a simple but highly sophisticated system to efficiently manage the available resources within the network and wireless devices is a very crucial and extremely important issue to be addressed.

Multiobjective optimization has been applied to many different fields to solve complex problems [12]. To the best of the authors' knowledge, little research has been done on the application of multiobjective particle swarm optimization to wireless video streaming. This paper explores the potential application of the aforementioned optimization scheme in wireless multimedia communication since there is a need to enhance system performance and manage resources efficiently. Interestingly, bioinspired algorithms have the capability to significantly improve the performance of wireless communication networks due to their dynamic features, such as adaptability, stability, and simplicity – which eventually reduce the computational complexity. The proposed multiobjective cross-layer optimization scheme is based on particle swarm optimization (PSO). PSO [13], [14], [23] dramatically reduces the computational time when compared to other optimization techniques and can be extremely useful for delay constraint applications such as video streaming. PSO is a well-known bioinspired optimization technique that is based on a simple model of bird flocking.

Much of the research effort on multiobjective optimization focuses on different techniques to achieve optimal performance. More importantly, many PSO schemes have been used in solving different multiobjective problems [31]–[33]. In [34], the authors proposed a PSO-based approach that induces stability to allow identification of optimal solutions and also to ensure effective distribution of decision and

objective spaces. Xue *et al.* [15] proposed an approach for feature selection using PSO to ultimately enhance performance. Reference [16] used decomposition to simplify the multiobjective optimization problem by scaling the multiple problems into sub-problems and taking into consideration the information from neighboring sub-problems. In [17], variable length PSO has been proposed for feature selection by enabling particles to have different lengths to improve the PSO and classification performance. The scheme can skip local optima and move toward more effective solutions. Furthermore, [18] proposed an adaptive local searching approach, which will ensure fast convergence when dealing with multimodal function problems, which are complex in nature and difficult to be solved in optimization.

Khan *et al.* [35] proposed a joint optimization scheme, which considers the application, data link, and physical layer to maximize user satisfaction in hiperLAN. Additionally, Huh *et al.* [36] demonstrated that CLD can be applicable to real-time streaming for pre-encoded video with different clients in wireless networks using code division multiple access (CDMA). In [39], rate-distortion optimization was utilized to solve the problem of video streaming over packetized media. In addition, [45] proposed a cross-layer design approach that allows optimization of perceptual quality for delay constraint video transmission and ultimately ensures channel adaptation, which provides a tradeoff between playback and quality. Choi *et al.* [37] presented a technique for abstracting parameters from application, data link, and physical layers to deliver video over multiuser environments. In [38], similar approaches have been reported. The scheme proposed in [44] maximizes the perceptual video quality of the video stream through QoS mapping. More importantly, fair distribution amongst the end users is also accomplished. In [40], a joint cross-layer optimization scheme is proposed to enhance video quality and to reduce the complexity by off-line training. Reference [41] proposed a multiobjective optimization approach that uses dynamic programming and Lagrangian relation to select the best video quality and content coverage to meet up with the delay constraint. In addition, [54] has proposed a structural similarity (SSIM)-based approach that considers the dynamics of the transmission environment and perceived video quality to support effective video streaming over wireless. Furthermore, [48] proposed a cross-layer approach for subcarrier assignment to maximize the information rate and video quality for MU-MIMO OFDMA to support video communications.

The proposed scheme is primarily aimed at improving video quality in wireless environments by keeping track of the channel condition and to strategically adapt to achieve an optimal streaming rate. Our approach to wireless video streaming problems is entirely different from other schemes; we formulated the video streaming rate maximization and used multiobjective particle swarm to solve the optimization problem. Second, the source rate is adjusted based on the packet error rate and packet delay. The performance of the proposed multiobjective cross-layer particle swarm

optimization algorithm is evaluated and investigated using high, medium and low motion video samples to evaluate its efficiency.

The remainder of this paper is organized as follows: Section 2 mainly focuses on the concept of PSO and related work. Section 3 describes the multiobjective optimization problem and its mathematical foundation. The performance of the proposed multiobjective cross-layer particle swarm optimization algorithm is analyzed, simulated and investigated in Section 4. Finally, conclusions are provided in Section 5.

II. PARTICLE SWARM OPTIMIZATION

PSO is alarmingly becoming an important optimization tool, with applications ranging from neural network training [42] to control and engineering [43] due to aforementioned features. Bioinspired algorithms have developed mainly based on the successful evolutionary behavior of natural systems, which naturally mimic nature and adapt dynamically with the environment. These algorithms can be used in solving complex problems with high precision and sophistication due to their unique characteristics. The ability to mimic the behavior of ant colonies, bird flocking, fish schooling, honeybees, bacteria and animal herding is an extremely useful tool in tackling optimization problems with high precision and sophistication. In fact, PSO is very fast in terms of convergence and simple to implement when compared to other algorithms [27]. It is very obvious that to enhance the performance of wireless multimedia applications, many parameters and factors should be considered. Hence, multiobjective optimization PSO can eventually solve a variety of multiobjective problems to achieve optimal performance [28]. More importantly, multiobjective PSO can effectively search and determine the set of optimal solutions simultaneously. The wireless channel characteristic can be represented by highly non-linear objectives and constraints to genuinely consider its impact on the transmitted data or information.

Particle swarm optimization uses stochastic search to solve the optimization problem, which has been a very efficient and powerful tool for searching the optimal solution to a given particular problem. In general, most problems used to have one objective function, but due to conflict between the objective functions, there is need for multiobjective optimization to determine the best possible solution. Therefore, PSO can solve a multiobjective optimization problem since it can search the multidimensional space. The set of solutions produced are all potential solutions to the multiobjective optimization problem. Problems dealing with multiple objective function can be solved using multiobjective PSO with relative ease and high searching capability for optimum solutions [19], [53]. More importantly, it is computationally inexpensive due to its low complexity and memory requirement, which is good for delay constraint applications. Multiobjective PSO can be used in wireless networks to dynamically adapt with the environment to support multimedia applications and services.

Furthermore, it is very important to note that each particle represents a potential solution and its changes according to previous experience. For instance, if it has been assumed that the search space is n -dimensional with i number of particles, this can be represented as n -dimensional vector $\mathbf{X} = (x_1, x_2, \dots, x_n)^T$. The change in velocity of the particles can be expressed in terms of vector $\mathbf{V} = (v_1, v_2, \dots, v_n)^T$. In addition, the best position of the particles can be represented as $\mathbf{P} = (p_1, p_2, \dots, p_n)^T$. The velocity and position of a particle at time t can be represented by $v(t)$ and $x(t)$. More importantly, the velocity and position of the particle at time $t+1$ can be determined using the expressions in equations (1) and (2), respectively.

$$v(t+1) = \omega v(t) + c_1(p_1 - x(t)) + c_2(p_g - x(t)) \quad (1)$$

$$x(t+1) = x(t) + v(t+1) \quad (2)$$

where c_1 and c_2 are the acceleration coefficients, vector P_1 is the best previous position of particle, i known as the personal best position within the local search space, and vector P_g is the best position among the personal best positions of the particles in the population and is known as the global best position [29]. Generally, the value of $v(t+1)$ is restricted between $-v_{\min}$ and v_{\max} to confine the search space. The inertia weight ω is primarily introduced to accelerate the convergence speed of the algorithm [30].

The velocity equation can be simplified further as $v(t+1) = v(t) + \varphi(p-x(t))$. In addition, we can represent equation (1) as $v(t+1) = v(t) + \varphi k(t)$, where $k(t) = p-x(t)$. The velocity and position equations at time $t+1$ can be represented in conical form as shown in equation (3)

$$\begin{bmatrix} v(t+1) \\ k(t+1) \end{bmatrix} = \begin{bmatrix} 1 & \varphi \\ -1 & 1 - \varphi \end{bmatrix} \begin{bmatrix} v(t) \\ k(t) \end{bmatrix} \quad (3)$$

Essentially, equation (3) relates the velocity and update of the particles at time $t+1$. The learning factors are represented by φ to simplify equations (1) and (2).

III. VIDEO-AWARE QOS PROBLEM FORMULATION

A. VIDEO-AWARE QOS MODEL

The optimization problem is primarily aimed at improving video quality and reducing delay. Hence, the parameters considered primarily include delay and packet error rate. Determining the optimal solution for these parameters can reasonably maintain video quality and reduce packet loss and computational complexity. Therefore, we represent the problem using decomposition theorem, which is purely based on divide and conquer. Figure 1 shows the typical strategy used to solve the multiobjective problem for wireless video streaming.

In general, decomposing the video streaming problem into sub-programs helps tremendously in the design by dividing the problem into layers or elements. In this case, vertical decomposition is considered to control multiple functions or layers. It is a known fact that vertical decomposition is used for joint control applications [20], [21]. Minimizing delay and packet error rate improves the network performance

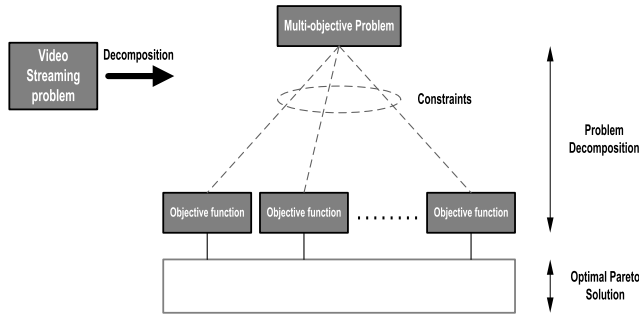


FIGURE 1. Typical wireless video streaming multi-objective problem.

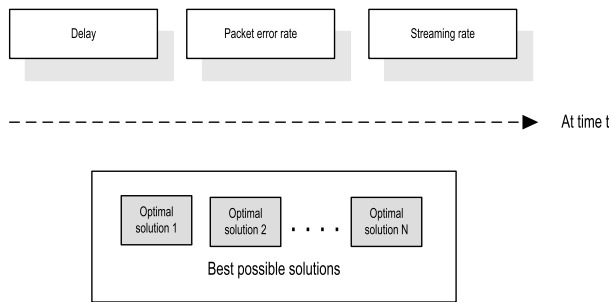


FIGURE 2. Multiobjective problem decomposition.

and video quality. The scheme is aimed at ensuring optimal throughput so that video quality is maintained in time-varying channel condition.

The multiobjective PSO problem can be decomposed into a sub-objective function to reduce complexity and to simplify the problem. To achieve this goal, two main parameters were selected to optimally support video streaming over wireless networks. These parameters include packet error rate and delay. The above problem can be further split into sub-functions as shown in Figure 2, and each sub-objective function represents the parameters needed to achieve optimal video streaming quality.

B. VIDEO-AWARE QOS OPTIMIZATION PROBLEM

The problem can be represented as $G=(N,L)$, where N denotes the set of nodes, and L is the set of communication links connecting the nodes together. The modulus of N and L can be used to represent the number of nodes and links interconnecting the nodes. It has been assumed that S is the sets of video sources through which nodes stream the video content and $L(s)$ is the link used by the source s . Additionally, the video sources that send the streaming content via the link l can be represented as $\{s \in S \mid l \in L\}$. For any source to stream the video content, the packets are first queued in the buffer before they are served. The delay anticipated after the source places a request for the video content is termed as τ , where $\tau = \{\tau_1, \dots, \tau_n\}$. The total delay D_m can be computed by summing the queue waiting and transmission times. The packet error changes as the channel condition varies and can be represented as a set, where $P = \{p_1, \dots, p_n\}$. The packet

error rate P should be less than the maximum packet error rate (PER_m), and hence, the link quality between the source and node can be determined. Based on the aforementioned scenario, the problem can be formulated and presented mathematically as follows:

$$\vartheta = \mathbf{arg\ min} \psi(P, \tau) \tag{4}$$

Subject to :

$$\tau \leq D_m$$

$$P \leq PER_m$$

$$x_l \geq 0 \tag{5}$$

Equation (4) is the utility function, which comprises two functions, namely, packet error rate p_i and delay τ_i . The constraints are represented by equation (5), which ensures that all the parameters are computed within the packet deadline and the maximum packet error rate is not exceeded. Additionally, the available link rate should be greater than zero (i.e., $x_l \geq 0$).

For multiobjective optimization problems, two main objectives need to be achieved at the shortest possible packet deadline. Computing the minimum average delay and packet error rate based on the media content (video) and network condition will provide the necessary QoS to achieve optimal performance within the network. Multicriteria decisions are implemented at the base station due to fact that the video packets to be transmitted can be effectively controlled from the source. More importantly, it has more processing power for fast computation when compared to mobile devices.

Objective

- Minimize the delay to meet with the application deadline
- Minimize the total number of packets lost
- Maximize the streaming rate by reducing the delay and packet error rate

Constraint

- Packet deadline constraint has been considered
- Packet error rate constraint

Suppose that the above objectives and constraint functions can be differentiated continuously, and the optimal condition for the multiobjective optimization can be represented in a first or second partial differential equation. For simplicity, we consider the first-order optimality condition. Therefore, the necessary condition for pareto optimal can be described as in [24]. It is very important to note that the necessary condition for x^* to be pareto optimal is that there are vectors $\vartheta_i \geq 0$ and $u_i \geq 0$ such that the following conditions are true:

$$\sum_{i=1}^l \vartheta_i \nabla f_i(x^*) - \sum_{k=1}^K \vartheta_k \nabla f_k(x^*) = 0 \tag{6}$$

$$u_k g_k(x^*) = 0 \quad \text{for all } k = 1, 2, \dots, K \tag{7}$$

For an unconstraint multiobjective optimization, the constraint portion of equation (6) can be neglected, which subsequently yields equation (8):

$$\sum_{i=1}^l \vartheta_i \nabla f_i(x^*) = 0 \tag{8}$$

The vector can be represented in matrix form if it has N objective and n variables.

$$\begin{bmatrix} \frac{\partial^k f_1}{\partial x_1^k} & \cdots & \frac{\partial^k f_N}{\partial x_1^k} \\ \vdots & \ddots & \vdots \\ \frac{\partial^k f_1}{\partial x_n^k} & \cdots & \frac{\partial^k f_N}{\partial x_n^k} \end{bmatrix} \begin{bmatrix} \vartheta_1 \\ \vdots \\ \vartheta_n \end{bmatrix} = \begin{bmatrix} 0 \\ \vdots \\ 0 \end{bmatrix} \quad (9)$$

In a situation where by n is equal to N , the pareto optimal solution should satisfy the following determinant condition:

$$\begin{vmatrix} \frac{\partial^k f_1}{\partial x_1^k} & \cdots & \frac{\partial^k f_N}{\partial x_1^k} \\ \vdots & \ddots & \vdots \\ \frac{\partial^k f_1}{\partial x_n^k} & \cdots & \frac{\partial^k f_N}{\partial x_n^k} \end{vmatrix} = 0 \quad (10)$$

In addition, the determinant should always be zero to determine the pareto optimal solution.

C. OPTIMALITY CRITERIA

To determine the pareto optimal for the multiobjective optimization with constraint, the minima of the objective function $f(x)$ can be determined depending on what is to be achieved. It is essential to analytically define the scheme to test the optimality of a given solution. Hence, the scheme can be defined analytically using the procedure described by the mathematical expression in equation (11). The optimal stream rate problem can be represented mathematically as follows:

$$\text{Minimize } f(x) = \sum_{l=L} \psi(P, \tau)$$

Subject to:

$$\begin{aligned} \sum_{l=L} \tau_l &\leq D_M \quad \forall l \in L \\ \sum_{l=L} P_l &\leq PER_M \quad \forall l \in L \\ x_l &\geq 0 \quad \forall l \in L \end{aligned} \quad (11)$$

Basically, the problem can be represented by equation (12) as follows:

$$\begin{aligned} L(I, x, \lambda) &= \sum_{l \in L} \psi(P, \tau) + \sum_{l \in L} x_l \left(\sum_{l \in L} \tau_l - D_M \right) \\ &+ \sum_{l \in L} \lambda_l \left(\sum_{l \in L} P_l - PER_M \right) \\ &= \sum_{l \in L} \psi(P, \tau) + \sum_{l \in L} x_l \sum_{l \in L} \tau_l - \sum_{l \in L} x_l D_M \\ &+ \sum_{l \in L} \lambda_l \sum_{l \in L} P_l - \sum_{l \in L} \lambda_l PER_M \\ &= \sum_{l \in L} \left(\psi(P, \tau) + \tau_l \sum_{l \in L} x_l + P_l \sum_{l \in L} \lambda_l \right) \\ &- \sum_{l \in L} x_l D_M - \sum_{l \in L} \lambda_l PER_M \end{aligned} \quad (12)$$

If $q_l = \tau_l \sum_{l \in L} x_l + P_l \sum_{l \in L} \lambda_l$, the equation above can be re-written as

$$= \sum_{l \in L} (\psi(P, \tau) + q_l) - \sum_{l \in L} x_l D_M - \sum_{l \in L} \lambda_l PER_M \quad (13)$$

where $q = [q_1, q_2, \dots, q_l]$, and hence, the Lagrange of the dual function to the optimization problem can be represented mathematically as follows:

$$\begin{aligned} G(I, x, \lambda) &= \min(L(I, x, \lambda)) \\ &= \min \left(\sum_{l \in L} (\psi(P, \tau) + q_l) - \sum_{l \in L} x_l D_M - \sum_{l \in L} \lambda_l PER_M \right) \end{aligned} \quad (14)$$

By setting equation (14) to zero and re-arranging the terms in the equation, it eventually yields:

$$\sum_{l \in L} (\psi(P, \tau) + q_l) = \sum_{l \in L} x_l D_M + \sum_{l \in L} \lambda_l PER_M \quad (15)$$

The update of the dual variables is achieved using equations (16) and (17), as shown below:

$$x_l^{(n+1)} = \min \left(x_l^{(n)} - \theta^{(n)} \left(D_M - \sum_{l \in L} \lambda_l \right) \right), \quad \forall l \in L \quad (16)$$

$$\lambda_l^{(n+1)} = \min \left(\lambda_l^{(n)} - \theta^{(n)} \left(PER_M - \sum_{l \in L} P_l \right) \right), \quad \forall l \in L \quad (17)$$

where $\theta^{(n)}$ is the step size at nn iteration, and it should be greater than zero. The values of x and λ can be computed at any particular time $(t+1)$ using the mathematical expressions in equations (16) and (17), respectively.

Hence, the optimal streaming rate can be expressed as follows:

$$\begin{aligned} R_{opt} &= \zeta T_f (1 - \min(\psi)) \\ &= \zeta T_f \left(1 - \min \left(\alpha \cdot \frac{1}{N} \sum_{i=1}^N (p_1 - p_{i-1}) \right. \right. \\ &\quad \left. \left. + \beta \cdot \frac{1}{N} \sum_{i=1}^N (\tau_1 - \tau_{i-1}) \right) \right) \end{aligned} \quad (18)$$

where the optimal streaming rate depends on the packet error rate and the delay anticipated within the network. The product of the minimum optimal computed packet error rate and delay is represented by ψ , as shown in equation (18), and ζT_f represents the packet arrival rate. The optimal streaming rate R_{opt} can be achieved when ψ is negligible, and it is represented by the terms shown in equation (18) above. R_{opt} has to satisfy the necessary constraints attached to the optimization problem. The mathematical formulation clearly shows that the optimal streaming rate can be obtained by minimizing the delay and packet error rate in the network, at the same time conforming to the packet deadline requirement of the streaming application.

D. BIOCOOPERATIVE VIDEO-AWARE QoS CROSS-LAYER OPTIMIZATION ALGORITHM

The algorithm below elaborates more on the bioinspired video-aware QoS multiobjective cross-layer optimization algorithm using PSO. More importantly, it clearly shows how the local and global bests of the objective functions are computed. The conceptual difference between the local and global best algorithms is the size of the neighborhood. In multiobjective PSO, the functions are related through the personal global best for each function. In a nutshell, the global best P_g computed in the first objective function is substituted into the v_d and vice versa. The goal is mainly to establish a relationship between the two objective functions. Logically, the packet error rate and delay are very much related such that a greater delay will result in higher packet error rate. Hence, these parameters can be used in developing the multiobjective optimization problem for a multimedia streaming application over a wireless network. By identifying the relationship between delay and packet error rate, it can be used in formulating the mathematical expression to determine the optimal streaming rate as it has been described in equation (18). The fitness for both the delay and packet error rate objective functions is represented as $\psi = \alpha \cdot \frac{1}{N} \sum_{i=1}^N (p_1 - p_{i-1}) + \beta \cdot \frac{1}{N} \sum_{i=1}^N (\tau_1 - \tau_{i-1})$.

The objective function described above consists of the packet error and delay components. Hence, it can be represented by ψ . α and β represent the weight attached to the packet error and delay components in the objective function. The sum of α and β both should be unity. To ensure fairness, both α and β have been set to 0.5. Therefore, the packet error rate and delay have the same weight, which implies that each of the parameters has been fairly given equal priority in regard to decision making for the optimal solution to the problem.

In a nutshell, the algorithm for the multiobjective cross-layer optimization using particle swarm can be represented as follows:

E. COMPLEXITY ANALYSIS

In this section, the complexity of the algorithm has been evaluated both numerically and experimentally. There has not been any technique to map the complexity of an algorithm and the power consumed as a result of using the algorithm. The computational complexity can be used as a metric to predict the power consumption. The actual time used by the central processing unit (CPU) to execute the algorithm can be used to measure its complexity. Hence, we adapt this technique to measure the complexity of the developed algorithm. The computational complexity is a measure used to determine the efficiency or capability of an optimization technique to find an optimal solution or terminate. Computational complexity is the measurement of the time needed to solve the multiobjective problem. It is very important, especially while dealing with applications that are sensitive to delay. This has been used to characterize the nature of the problem and determine

Algorithm 1 Biocooperative Video-Aware QoS Cross-Layer Optimization Algorithm

Objective: To maximize the video streaming rate based on the packet error rate and delay

01. Initialize the size of the particle swarm n , and other parameters
02. Initialize swarm with random positions and velocities of n particles
03. While (ending criteria has not been reached) do
04. For $i = 1$ to n
05. Compute the packet error rate P_i and delay τ_i at time t
06. Check if $\sum_{l \in L} \tau_l \leq D_M$ and $\sum_{l \in L} P_l \leq PER_M$
07. Determine the new position & velocity
08. Select local and global bests
09. Compute the fitness $\psi = \alpha \cdot \frac{1}{N} \sum_{i=1}^N (p_1 - p_{i-1}) + \beta \cdot \frac{1}{N} \sum_{i=1}^N (\tau_1 - \tau_{i-1})$
10. If the current fitness of the particle is less than the previous, replace the previous with the new fitness
11. Update particle velocities and positions as follows:

$$v(t+1) = \omega v(t) + c_1(P_1 - x(t)) + c_2(P_g - x(t))$$

$$x(t+1) = x(t) + v(t+1)$$
12. end
13. end
14. end
15. Increase the loop counter, $i+1$
16. end // once stopping condition has been reached;
17. Output $\vartheta = \mathbf{arg\ min} \psi(P, \tau)$

whether it can be solved within the time frame. In addition, this has provided the evidence for using PSO to solve the multiobjective cross-layer optimization problem. It is obvious that complex problems are difficult to solve, and finding such a solution is costly in terms of time and space.

The computational time is juxtaposed with the packet deadline of the application to determine if the optimization algorithm can be able to converge within the speculated period of time. Based on the numerical analysis, it has been established that many parameters can culminate to increase the computational complexity of the scheme apart from the fitness function that describes the algorithm. The computational complexity of a PSO-based bioinspired algorithm depends mainly on the number of the objective functions, particles and constraints. The algorithm complexity can be characterized and represented graphically as a linear, quadratic or higher-order system. Hence, the complexity of the optimization can be represented diagrammatically as shown in Figure 3. As seen, the computational time increases as the number of functions and constraint increase.

To analytically evaluate the complexity of the developed scheme based on the computational time, we first assumed that the objective functions f and constraints have been known. The multiobjective optimization problem can be

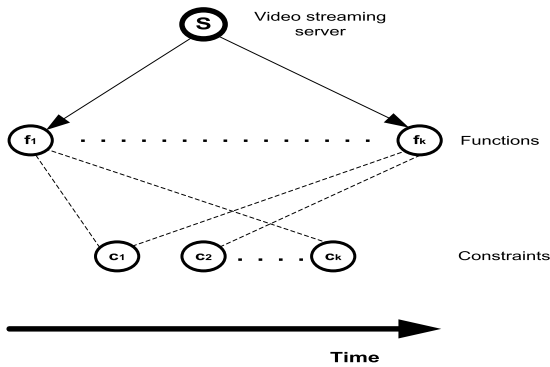


FIGURE 3. Timing diagram for computational complexity.

represented as $f = (f_1 \dots f_k)$, and it is assumed to be represented by a vector $f : S \rightarrow R^k$. The quality of the output of the search result with order R^k can be expressed as $f(s) \leq f(s')$ iff $f_i(s) \leq f_i(s')$ for all $i \in \{1, \dots, k\}$. The value of $f(s)$ is minimal with respect to the partial order and $f(s')$, and the pareto optimal search point can have different objective vectors.

In general, equation (21) can be used to determine the computational complexity numerically, but it is not as accurate as using time lapse to execute the tested algorithm. This is mainly because the complexity of one function is different from another. Hence, the general formula to determine the complexity can be formulated and mathematically represented as follows. Based on the experiment, it has been assumed that the complexity $c_i = \{m_i, n_i^2\} \in C_i$ for $i = 1, \dots, K$, as the complexity vector for the set of complexity strategy vectors to perform a particular task. where $C_i = N_i \times M_i$ and $M_i = \{m_1, \dots, m_k\}$ and $N_i = \{n_1^2, \dots, n_k^2\}$.

It is obvious that the algorithm will determine the optimal value in time proportional to the k number of objective functions. As the number of constraints increases, the computational complexity will also increase. This has been described in Figure 3, which clearly shows that the computational time increases with an increase in the number of objective functions. In this case, two objective functions are considered for the optimal video streaming problem. Figures 4, 5 and 6 show the complexity analysis while using 2 to 4 objective functions to solve the multiobjective problem based on the developed algorithm. The graphs show that the proposed algorithm seems to be exponential, which can be represented as $O(MN^2)$. The complexity depends on the numbers of particles and objective functions. As shown in Figures 4, 5 and 6, the computational time increases exponentially as the numbers of particles and objective functions increase. The complexity C is given by the product of M and N^2 . The maximum computational complexity of the optimization problem can be obtained by differentiating MN^2 with respect to N , and it can be expressed mathematically as follows:

$$\frac{\partial C}{\partial N} = \frac{\partial}{\partial N} (MN^2) = 2MN \quad (19)$$

The maximum achievable computational time with respect to the number of particles and the number of

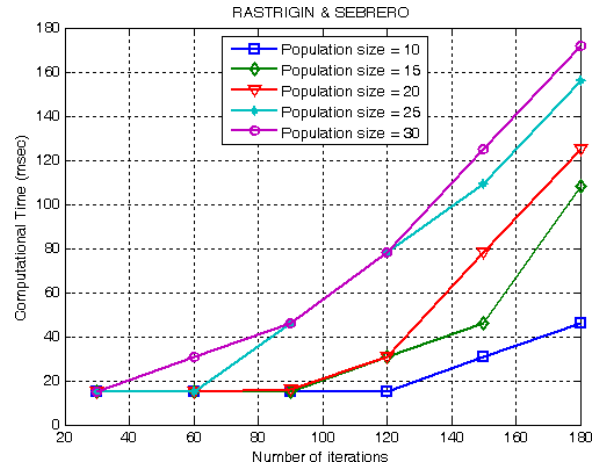


FIGURE 4. Computational complexity for two objective functions.

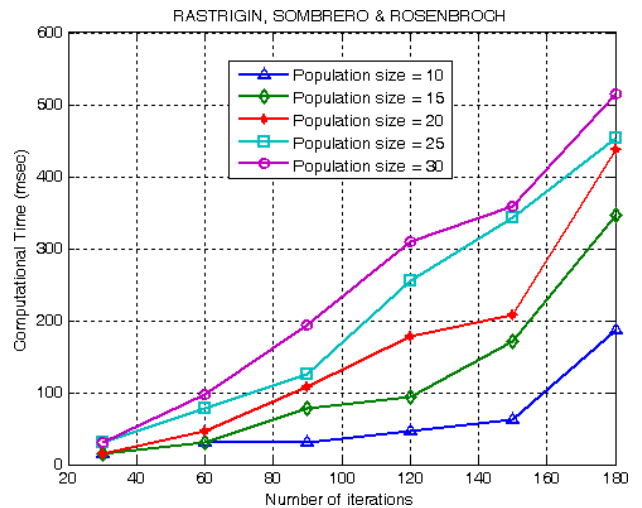


FIGURE 5. Computational complexity for three objective functions.

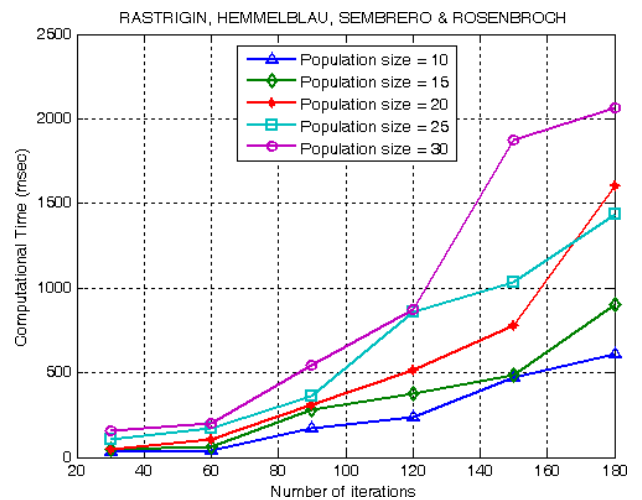


FIGURE 6. Computational complexity for four objective functions.

objectives can be obtained and represented as shown in equations (19) and (20), respectively.

$$\frac{\partial C}{\partial M} = \frac{\partial}{\partial M} (MN^2) = N^2 \quad (20)$$

In both equations (19) and (20), it is clearly indicated that the number of particles contributed greatly toward increasing the computational complexity of the optimization problem. Therefore, the number of particles has been strategically selected through numerical analysis.

Additionally, the complexity of the optimization algorithm [24] can be computed using equation (21). As can be noted, the complexity depends greatly on the number of objective functions and the number of particles. Therefore, the complexity increases increasing M and N :

$$O(MN^2) \quad (21)$$

where M is the number of objective functions and N represents the number of particles. In this work, the number of particles is determined experimentally and has been assigned to 30 to suit the application requirement.

IV. SIMULATION RESULTS AND ANALYSIS

The proposed MO-CLD scheme has been developed and studied using an NS-2 simulation environment. The performance of MO-CLD is analyzed and compared with the B-CLD scheme under different video traffic and settings. The performance metrics, such as video quality, end-to-end delay and buffer queue size, were used in evaluating the developed biocooperative video-aware QoS multiobjective cross-layer optimization algorithm. More interestingly, different scenarios have been used to measure the performance of the developed scheme to thoroughly determine its efficiency when subjected to different conditions.

A. SIMULATION SETUP

In the simulation of the proposed cross-layer approach, the IEEE 802.11b MAC and physical layer protocols have been adapted in the wireless LAN model [26]. The video samples (Hall, News and Coast Guard) used for the simulation are encoded using H.264. The video model used for the experiment primarily consists of an I-frame and a 14 P-frame. All three (3) QCIF (176×144) video samples are encoded with the same group structure for the video streaming application. Therefore, the pattern of the encoded frames is IPPPP...PPPIPPP, and in between each I-frames, there are 14 P-frames. The distance between two I-frames is termed as the group of pictures (GOP). The first frame in the group of frames is represented as i . The group can be represented by $G = \{i, i+1, \dots, (i+n-1)\}$, where n is the total number of frames in the group.

The optimization parameters have been set based on the particle swarm parameter configuration. The population size and total number of iterations were set to 30. The cognitive c_1 and social c_2 constants have been set to 1. The multiobjective optimizer has been tested using different objective functions to determine its efficiency and capability as the number of objective functions increases. In addition, the impact of increasing the number of iterations on the fitness value has been investigated to identify the number of iterations required to achieve optima and also conform to the delay constraint for

TABLE 1. PSO parameter settings.

Parameter	Value
Number of particles	30
Number of iteration	30
Learning factors c_1 & c_2	1
Inertia weight ω	0.5

TABLE 2. Simulation parameters.

Parameter	Value
Propagation model	Shadowing
PhyType	Phy/WirelessPhy/802_11
MacType	Mac/802_11
Freq	2.4 GHz
Data rate	1 – 11 Mbps
CSThresh	1-13
RXThresh	1.10765e-11
Video Samples (QCIF)	Hall, News & Coast Guard
Number of frames	300
GOP size	15
Frame size	176 x 144

TABLE 3. System specifications.

Characteristic	Description
CPU Type	Intel Pentium 4
Memory	1 GB
Operating system	Linux
Processor speed	1.7 GHz

multimedia applications. Based on the experimentation, it has clearly shown that the number of iterations to conveniently meet the delay requirement is 30 iterations, and the PER has been set to 0.01 [5].

The parameters and settings shown in Tables 1, 2 & 3 were used in developing and simulating the MO-CLD scheme.

B. VIDEO QUALITY

Maintaining video quality is a crucial issue in wireless LAN, as the optimization scheme ensures that maximum video quality is achieved at the destination. The fact is that the optimization process will require time to determine the optimal solution, but it still depends on the efficiency of the optimization scheme. The developed scheme is compared with the B-CLD. In the B-CLD, the decision algorithms to stream video traffic on the wireless medium are based on threshold values. B-CLD uses queue and delay statistics and subsequently adjusts the transmission rate to meet up with the constraints of the video content. Although the scheme is adaptive, the computational time is greater when compared to MO-CLD.

Video quality is measured by comparing the original and reconstructed video signals based on the peak signal to noise ratio ($PSNR$), which presents the objective video quality of

TABLE 4. Video quality comparison.

	Hall (dB)	News (dB)	Coast Guard (dB)
B-CLD	32.95	32.62	29.78
MO-CLD	33.72	32.84	29.95

each video frame by a single number. The mean square error (*MSE*) for each frame is converted to *PSNR* by mapping the 8-bit original signal. The actual difference or loss in video quality can be determined using equation (22):

$$PSNR = 10 \log_{10} \left(\frac{255^2}{MSE} \right) \quad (22)$$

where the *MSE* can be computed using the formula in equation (23):

$$MSE = \frac{1}{W * Z} \sum_{i=0}^{W-1} \sum_{j=0}^{Z-1} (Y_s(i, j) - Y_D(i, j))^2 \quad (23)$$

$Y_S(i, j)$ represents the original source frame, and $Y_D(i, j)$ is the reconstructed frame at the destination, which contains $W * Z$ pixels. The video frame is composed of $W * Z$ pixels (for QCIF format, $W = 176$ and $Z = 144$). The larger the difference between the $Y_S(i, j)$ and $Y_D(i, j)$, the lower the *PSNR* value and vice visa.

More interestingly, it can be seen that the improvement varies from one type of video sequence to another, but they are all subjected to the same network condition and delay. The video quality has been improved by 0.77, 0.22 and 0.17 dB for low, medium and high motion sequences, respectively, as shown in Table 4. This is attributed to the fact that many features of CLD have been used in developing MO-CLD, and the optimization scheme is the major conceptual difference between the two schemes used to enhance the QoS over the wireless network. The packet error rate and delay have been reduced by adapting to the condition of the channel and strategically adjusting the streaming rate. It is very clear that the improvement in video quality decreases as the video sequence motion and scene complexity increase.

The comparison in Table 4 is represented graphically in Figures 7, 8 and 9. The comparison clearly shows the variation in video quality for the three (3) video sequences used for the experimentation. The developed MO-CLD scheme has been tested using different video test sequences to verify the performance of the strategy in terms of *PSNR*. Table 4 shows the comparison between MO-CLD and B-CLD for Coast Guard, News and Hall sequences. In a nutshell, the improvement in video quality increases with a decrease in complexity. The proposed MO-CLD scheme shows better results than B-CLD, but the video improvement depends mainly on the type of video motion and scene complexity. In addition, it can be concluded that motion and scene complexity play an integral role in maintaining the video streaming quality.

As seen from Figures 7, 8 and 9, it is very obvious that the MO-CLD has been able to consistently maintain the

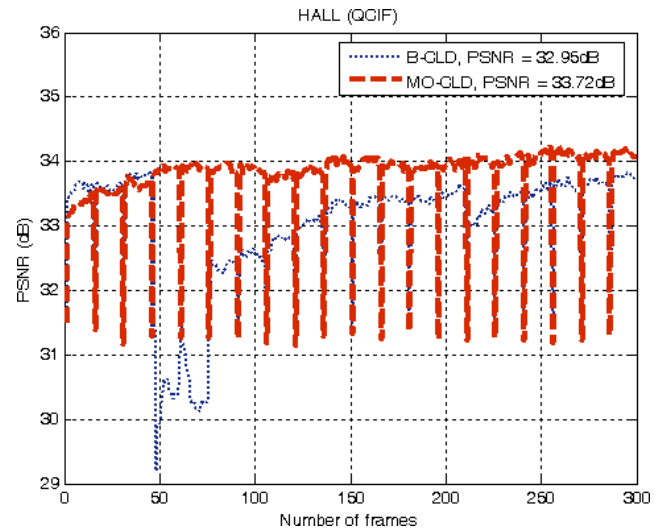


FIGURE 7. Video quality comparison between B-CLD and MO-CLD, Low motion sequence: HALL (176 × 144 @ 30fps).

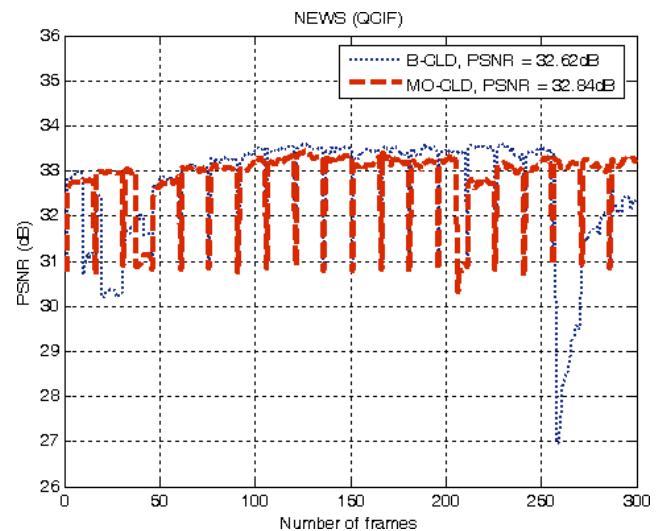


FIGURE 8. Video quality comparison between B-CLD and MO-CLD, Medium motion sequence: NEWS (176 × 144 @ 30fps).

video quality above 29 dB despite the variation in channel condition. The proposed scheme uses *PER* and delay statistic in real time and subsequently adjusts the transmission rate to meet up with the constraint of the video content and frame type at any particular time. The Hall sample has exhibited better video quality when compared to the News and Coast Guard decoded video samples. This is mainly due to its low video complexity. More interestingly, the Hall video quality has been maintained close to 34 dB from the 50th to the 300th frame, as can be seen in Figure 7. For the News video sample, the video quality is maintained at approximately 33 dB from the 50th frame up to last frame in the video sample, as shown in Figure 8. Additionally, it can be clearly noted that the Coastguard sequence experiences low video quality while streaming over the same wireless medium as the Hall and News sequences. This is attributed to its high complexity nature. In a nutshell, the improvement in video quality

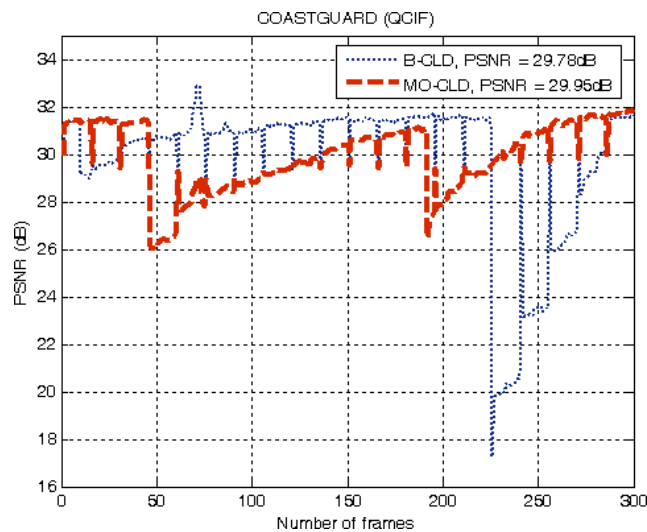


FIGURE 9. Video quality comparison between B-CLD and MO-CLD, High motion sequence: COASTGUARD (176 x 144 @ 30fps).

increases with a decrease in complexity. Although the video quality in the Coastguard sequence is affected by the channel condition, better video quality is achieved while using the MO-CLD scheme when compared to the B-CLD scheme.

Figure 10 shows the qualitative comparisons of the video quality on a frame-by-frame basis, and it can be observed that the video quality of the frames using the MO-CLD scheme outperform the B-CLD scheme when the video samples used for the experimentation were decoded and evaluated at the destination. The sample decoded videos using the MO-CLD scheme are presented on the left-hand side of Figure 10, while the sample videos using the B-CLD scheme are on right-hand side. Interestingly, the video samples used for the test show that MO-CLD can adapt to the rapid dynamics of the channel, and it provided the necessary QoS support for the streamed videos. The simulation work shows that the complex nature of the video samples can lead to delay – this can affect the performance of MO-CLD and B-CLD due to increases in computational complexity.

Since the primary object of the developed scheme is to maximize streaming rate while taking into consideration both the packet loss and delay to improve video quality, it is clear that both quality assessment tools and visual inspection have shown that MO-CLD has been able to accomplish better video quality when compared B-CLD. The next objective is to compare the proposed MO-CLD scheme and B-CLD in terms of effective buffer management.

C. BUFFER QUEUING SIZE

To effectively test the capacity of the proposed scheme, the network is subjected to the traffic generated by the video samples, and the queue size is monitored. The queue size was appropriately managed, which eventually culminated as low traffic and congestion within the network, and consequently increased the performance significantly. The queue size was relatively low when compared to B-CLD. In the News and



FIGURE 10. Decoded sample frames for the reconstructed videos (Hall, News, Coast Guard) for MO-CLD on the left and B-CLD on the right.

Hall video sequences in Figure 11, the queue size was evenly distributed over the period of time. In addition, the processing and queue management capability of MO-CLD outperform those of B-CLD since the queue size is efficiently managed to meet the QoS requirements and network conditions. This is attributed to the capacity of the optimization scheme to adapt to rapid variation in network parameters and act swiftly. Interestingly, MO-CLD is designed to support Ad-hoc networking with optimal streaming throughput to achieve high video quality. The traffic was managed appropriately, which reduced congestion and unnecessary packet dropping.

The Coastguard sequence is unique when compared to the other sequences in terms of pattern of the queue size, where for consecutive times, packets were delayed for a short period. Obviously, this effect was mainly the result of channel condition, and more packets were transmitted initially, and it posed when the channel condition deteriorated.

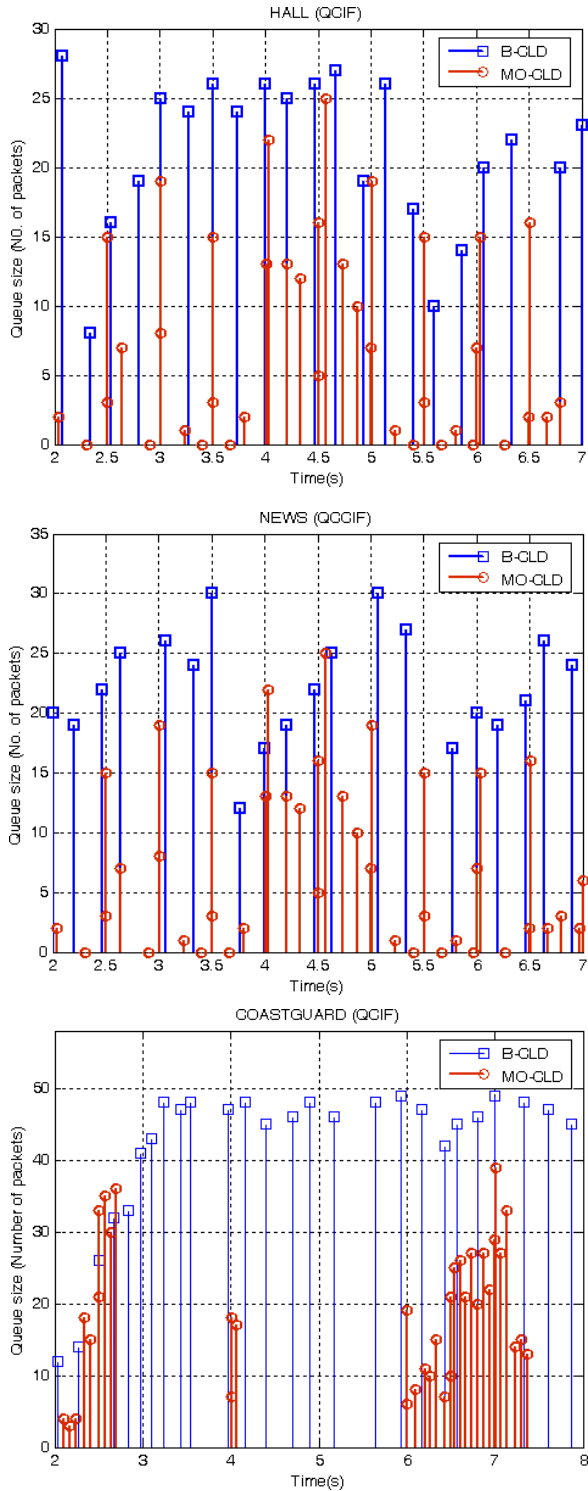


FIGURE 11. Queue size comparison between B-CLD and MO-CLD for Hall, News and Coast Guard video sequences.

Adaptability is one of the key features of PSO. More packets are transmitted when certain conditions are satisfied by the network. For instance, the proposed MO-CLD was able to adapt to the transmission rate while streaming the Coastguard sample video. From Figure 10, it can be seen that there were more packets in the queue between times $t=2s$ and $t=2.5s$.

Interestingly, packets were transmitted within the aforementioned period mainly due to good channel conditions, and the QoS requirements needed to support the high traffic were fulfilled.

In addition, it is clear that no packets were in the queue between $t=2.5s$ to $t=4s$ – this condition will lead to packet loss due to poor channel status. Furthermore, this behavior could be observed between $t=6s$ and $t=7.3s$, which indicated that there was more traffic on the queue, a clear indication of a good network condition and that packets are transmitted over the network. This shows the capability of the proposed MO-CLD to effectively manage the traffic based on the network condition. The developed MO-CLD scheme deploys this strategy when dealing with high traffic and complex video samples, which requires more efficient and effective queue management strategies. To clearly see the impact of the queue size on delay, the end-to-end delay is evaluated in the next section.

D. END-TO-END DELAY

End-to-end delay is used to measure the performance of the scheme to compare their performance in terms of latency. Although MO-CLD has to select the optimal parameters, its performance is better when compared to B-CLD. The delay was significantly reduced in all the sequences tested. This clearly demonstrates the efficiency of the scheme in terms of both high convergence capability and simplicity. The average delay was computed by deducting the time a packet is transmitted from the time the packet is received. In both cases, the delay was still within the time deadline for the video streaming application, but still more has to be done reduce the processing time to a minimum. It is very important to note that only propagation delay was considered in this analysis since the main focus of the research is on how to mitigate the impact of transmission errors on video streaming quality. In a nutshell, this feature for MO-CLD will be extremely useful in wireless multimedia network.

As can be seen from Figure 12, the end-to-end delays for the News and Hall video samples were relatively low while streaming using the MO-CLD scheme. The delay while streaming the Hall video sample was low at time $t=2s$ to $t=4s$, which leads to better video streaming quality. There was an increment in delay from $t=4s$ up to $t=5.25s$ due to traffic burst. In addition, the end-to-end delay decreased greatly from $t=5.24s$ upward. As a result of the deployment of the MO-CLD scheme, the average end-to-end delay for the Hall sample video was significantly reduced by 50.66%. Similarly, the average end-to-end delay for the News video sample was minimized by 22.83% while streaming using the MO-CLD scheme.

Figure 12 shows similar behavior exhibited by the Coastguard video sample as in Figure 11, which also reflected in its end-to-end delay performance evaluation. As mentioned earlier, high-traffic videos can be effectively handled by selecting the best streaming strategy based on the delay and packet error at every particular time t . Based on the constraints,

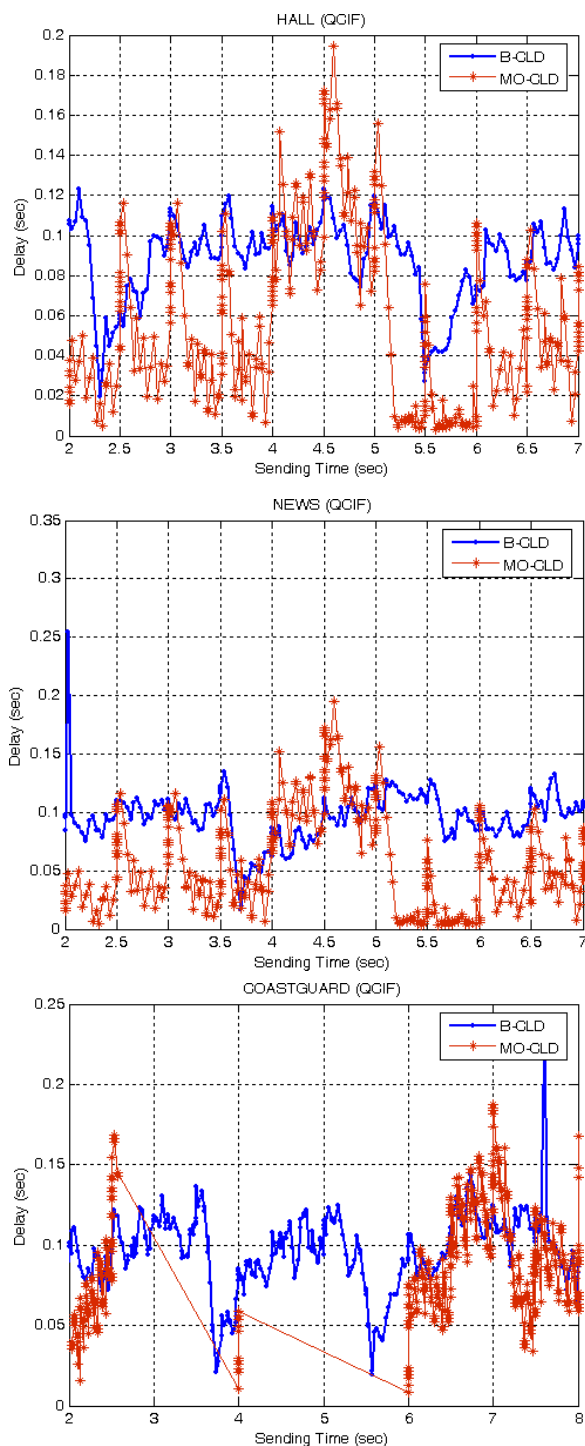


FIGURE 12. Delay vs Sending time comparison between B-CLD and MO-CLD for Hall, News and Coast Guard video sequences.

the optimal solution is determined, and the streaming rate is eventually adjusted. For instance, $\tau(t)$ is thoroughly checked and compared with $\tau(t-1)$ and D_m . The MO-CLD scheme always determines the best time period to transmit, and once that time period is established, it transmits the packets continuously until the channel condition worsens and becomes unreliable. The reason why there were no delay data within

TABLE 5. End-to-end delay comparison.

Sequence	MO-CLD	B-CLD	$\Delta T(\%)$
Coast Guard	0.078748	0.089904	12.40
News	0.065946	0.085461	22.83
Hall	0.043221	0.087600	50.66

the time period $t=2.5s$ to $t=3.9s$ and $t=4.1s$ to $t=5.9s$ is due to the unreliable wireless connectivity. Hence, no packet was transmitted, and the end-to-end delay was negligible. This situation could lead to packet loss and retransmission if packets are transmitted within those time periods. Consequently, it may increase the overall network delay as well. It can be seen that there was a data delay while streaming the Coastguard video sample at $t=6s$ and above, which indicated that the network condition had normalized and was suitable for transmitting the video packets. With the dynamics of the network and a high-traffic video (such as the Coast Guard video), it is difficult to manage such traffic, but PSO has successfully been used to make effective decisions since it has high convergence capability. For each of the sample videos, the average end-to-end delay was computed and is presented in Table 5.

The proposed biocooperative scheme has reduced the end-to-end delays by 50.66%, 22.83% and 12.4% for the Hall, News and Coast Guard video samples, respectively. Based on the simulation results, it can be concluded that the end-to-end delay increases with the increases in complexity and queue size. In summary, reducing the delay within the network will lead to reductions in packet drop and error; ultimately, it will significantly reduce the energy consumption as a result of processing, retransmission and computation.

The energy efficiency of the MO-CLD scheme is accomplished based on two important steps included in the biocooperative video aware QoS cross layer optimization algorithm: the first step determines the condition when τ_l and P_l meet up with the optimization criteria. Therefore, the algorithm is executed only in a situation when the constraints of the optimization problem in equation (5) have been satisfied – this avoids unnecessary execution of the algorithm. This eventually allows comparison of the computed average delay and packet error rate in time t with the maximum threshold values. More interestingly, it is very important to note that these two components are related to one another. The second step involves the use of PSO to select the best delay and packet error rate which will yield the optimal streaming rate when substituted into the fitness function. The energy saving ability of the scheme is accomplished by executing the two steps which in turn, reduced the complexity and consequently lead to low energy consumption in network since the energy and resources needed have been effectively managed. Intuitively, the QoS is dependent on the parameters τ_l and P_l . By deploying these two strategies, the network performance has been enhanced significantly.

Finally, the complexity between the proposed MO-CLD algorithm and the B-CLD algorithm was measured to

compare the energy efficiency of the schemes. It is obvious that more computational time will lead to more energy consumption. The simulation experiment was conducted on the system with specifications described in Table 3. The simulation test was primarily aimed at determining the efficiency of the two algorithms in terms of complexity. Therefore, the energy efficiency of the proposed scheme has been measured and compared with B-CLD in terms of time complexity. For each of the schemes, a high-complexity video (Coastguard) was used to test its complexity. The goal is to test and ensure how effective the developed scheme is using high-traffic and complex video samples. The computational times for the two schemes were tested online: the average processing time for MO-CLD was 15 ms while the processing time for the B-CLD scheme was approximately 85 ms. The computational complexity when using MO-CLD was significantly reduced by 82.3%, which clearly shows the energy efficiency of the developed algorithm when compared with B-CLD.

V. CONCLUSION

In this paper, we proposed an efficient multiobjective cross-layer optimization scheme using a biocooperative approach to optimally support wireless video streaming. This paper fundamentally presents a new design paradigm that improves video quality by effectively managing the end-to-end delay and the buffer queue size. First, the multiobjective problem was formulated and solved using a bioinspired approach. The proposed approach was analyzed both mathematically and using simulation to verify the performance of the bioinspired optimization scheme in terms of video quality and complexity. Considering the channel condition when transmitting the video packet reduced the possibility of retransmission to a minimum. More importantly, the throughput was maximized, which led to high video quality. The proposed bioinspired optimization algorithm for streaming applications is highly efficient and adaptive, which makes it suitable for video streaming applications in a time-varying changing environment. Extensive simulations have clearly shown an improvement in video quality compared to the B-CLD approach. Our future interest is to adapt this technique to develop a hybrid multiobjective cross-layer optimization for wireless multimedia communication.

ACKNOWLEDGMENT

This work was funded by the Deanship of Scientific Research (DSR), King Abdulaziz University, Jeddah, under grant no. DF-802-830-1441. The author, therefore, gratefully acknowledges the DSR technical and financial support.

REFERENCES

- [1] Y. Wu, S. Kumar, F. Hu, Y. Zhu, and J. D. Matyjas, "Cross-layer forward error correction scheme using raptor and RCP codes for prioritized video transmission over wireless channels," *IEEE Trans. Circuits Syst. Video Technol.*, vol. 24, no. 6, pp. 1047–1060, Jun. 2014.
- [2] M. F. Majeed, S. Hassan Ahmed, S. Muhammad, H. Song, and D. B. Rawat, "Multimedia streaming in information-centric networking: A survey and future perspectives," *Comput. Netw.*, vol. 125, pp. 103–121, Oct. 2017.
- [3] M. Van der Schaar and P. A. Chou, *Multimedia over IP and Wireless Network: Compression, Networking and Systems*. New York, NY, USA: Academic, 2007.
- [4] A. Zhou, M. Liu, Z. Li, and E. Dutkiewicz, "Cross-layer design for proportional delay differentiation and network utility maximization in multi-hop wireless networks," *IEEE Trans. Wireless Commun.*, vol. 11, no. 4, pp. 1446–1455, Apr. 2012.
- [5] N.-S. Vo, T. Q. Duong, H.-J. Zepernick, and M. Fiedler, "A cross-layer optimized scheme and its application in mobile multimedia networks with QoS provision," *IEEE Syst. J.*, vol. 10, no. 2, pp. 817–830, Jun. 2016.
- [6] J. Tang, W. P. Tay, and T. Q. S. Quek, "Cross-layer resource allocation with elastic service scaling in cloud radio access network," *IEEE Trans. Wireless Commun.*, vol. 14, no. 9, pp. 5068–5081, Sep. 2015.
- [7] E. Setton, T. Yoo, X. Zhu, A. Goldsmith, and B. Girod, "Cross-layer design of ad hoc networks for real-time video streaming," *IEEE Wireless Commun.*, vol. 12, no. 4, pp. 59–65, Aug. 2005.
- [8] Y. Xiao and M. van der Schaar, "Optimal foresighted multi-user wireless video," *IEEE J. Sel. Topics Signal Process.*, vol. 9, no. 1, pp. 89–101, Feb. 2015.
- [9] M. Van Der Schaar and S. S. N., "Cross-layer wireless multimedia transmission: Challenges, principles, and new paradigms," *IEEE Wireless Commun.*, vol. 12, no. 4, pp. 50–58, Aug. 2005.
- [10] S. Efazati and P. Azmi, "Effective capacity maximization in multi-relay networks with a novel cross-layer transmission framework and power-allocation scheme," *IEEE Trans. Veh. Technol.*, vol. 63, no. 4, pp. 1691–1702, May 2014.
- [11] Y. S. Baguda, N. Faisal, S. K. Yusof, S. H. Syed, R. Rashid, and K. Saleem, "Cross layer error-control scheme for video quality support over 802.11b wireless LAN," in *Proc. TENCON IEEE Region Conf.*, Nov. 2009, pp. 2–5.
- [12] J. Kennedy and R. C. Eberhart, *Swarm Intelligence*. Burlington, MA, USA: Morgan Kaufman, 2001.
- [13] A. P. Engelbrecht, *Computational Intelligence*. London, U.K.: Wiley, 2007.
- [14] S. Zhang, J. Xu, L. H. Lee, E. P. Chew, W. P. Wong, and C.-H. Chen, "Optimal computing budget allocation for particle swarm optimization in stochastic optimization," *IEEE Trans. Evol. Comput.*, vol. 21, no. 2, pp. 206–219, Apr. 2017.
- [15] B. Xue, M. Zhang, W. N. Browne, and X. Yao, "A survey on evolutionary computation approaches to feature selection," *IEEE Trans. Evol. Comput.*, vol. 20, no. 4, pp. 606–626, Aug. 2016.
- [16] J. Chen, J. Li, and B. Xin, "DMOEA-εC: Decomposition-based multiobjective evolutionary algorithm with the ε-constraint framework," *IEEE Trans. Evol. Comput.*, vol. 21, no. 5, pp. 714–730, Oct. 2017.
- [17] B. Tran, B. Xue, and M. Zhang, "Variable-length particle swarm optimization for feature selection on high-dimensional classification," *IEEE Trans. Evol. Comput.*, vol. 23, no. 3, pp. 473–487, Jun. 2019.
- [18] Y. Cao, H. Zhang, W. Li, M. Zhou, Y. Zhang, and W. A. Chaovalitwongse, "Comprehensive learning particle swarm optimization algorithm with local search for multimodal functions," *IEEE Trans. Evol. Comput.*, vol. 23, no. 4, pp. 718–731, Aug. 2019.
- [19] V. L. Huang, P. N. Suganthan, and J. J. Liang, "Comprehensive learning particle swarm optimizer for solving multiobjective optimization problems," *Int. J. Intell. Syst.*, vol. 21, no. 2, pp. 209–226, Feb. 2006.
- [20] M. Chiang, S. H. Low, A. R. Calderbank, and J. C. Doyle, "Layering as optimization decomposition: A mathematical theory of network architectures," *Proc. IEEE*, vol. 95, no. 1, pp. 255–312, Jan. 2007.
- [21] D. P. Palomar and M. Chiang, "A tutorial on decomposition methods for network utility maximization," *IEEE J. Sel. Areas Commun.*, vol. 24, no. 8, pp. 1439–1451, Aug. 2006.
- [22] F. Fu and M. van der Schaar, "Decomposition principles and online learning in cross-layer optimization for delay-sensitive applications," *IEEE Trans. Signal Process.*, vol. 58, no. 3, pp. 1401–1415, Mar. 2010.
- [23] Y. S. Baguda, N. Faisal, S. H. Syed, L. A. Latiff, S. K. Yusof, R. A. Rashid, and D. S. Shuaibu, "Low complexity PSO-based multi-objective algorithm for delay-constraint application," in *Proc. ICIEIS*, 2011, pp. 274–283.
- [24] K. Deb, *Multi-objective Optimization Using Evolutionary Algorithms*. Hoboken, NJ, USA: Wiley, 2008.
- [25] M. Rezapour and A. I. Perez-Neira, "A cross-layer approach to heterogeneous multi-user diversity with link adaptation," *IEEE Trans. Wireless Commun.*, vol. 6, no. 11, pp. 4038–4048, Nov. 2007.
- [26] *IEEE Standard for Information Technology-Telecommunications and Information Exchange Between Systems-Local and Metropolitan Area Network-Specific Requirements—Part 11: Wireless LAN Medium Access Control (MAC) and Physical Layer (PHY) Specifications*. Standard P802.11bb, 2007.

- [27] M. E. H. Pedersen and A. J. Chipperfield, "Simplifying particle swarm optimization," *Appl. Soft Comput.*, vol. 10, no. 2, pp. 618–628, Mar. 2010.
- [28] R. Kumar and N. Banerjee, "Multiobjective network topology design," *Appl. Soft Comput.*, vol. 11, no. 8, pp. 5120–5128, 2011.
- [29] C.-C. Chen, "Two-layer particle swarm optimization for unconstrained optimization problems," *Appl. Soft Comput.*, vol. 11, no. 1, pp. 295–304, Jan. 2011.
- [30] A. Nickabadi, M. M. Ebadzadeh, and R. Safabakhsh, "A novel particle swarm optimization algorithm with adaptive inertia weight," *Appl. Soft Comput.*, vol. 11, no. 4, pp. 3658–3670, Jun. 2011.
- [31] S. Lalwani, S. Singhal, and R. Kumar, "A comprehensive survey: Applications of multi-objective particle swarm optimization (MOPSO) algorithm," *Trans. Combinatorics*, vol. 2, no. 1, pp. 39–101, 2013.
- [32] B. Y. Qu, J. J. Liang, and P. N. Suganthan, "Nicheing particle swarm optimization with local search for multi-modal optimization," *Inf. Sci.*, vol. 197, pp. 131–143, Aug. 2012.
- [33] J. Tian, Y. Tan, J. Zeng, C. Sun, and Y. Jin, "Multiobjective infill criterion driven Gaussian process-assisted particle swarm optimization of high-dimensional expensive problems," *IEEE Trans. Evol. Comput.*, vol. 23, no. 3, pp. 459–472, Jun. 2019.
- [34] C. Yue, B. Qu, and J. Liang, "A multiobjective particle swarm optimizer using ring topology for solving multimodal multiobjective problems," *IEEE Trans. Evol. Comput.*, vol. 22, no. 5, pp. 805–817, Oct. 2018.
- [35] S. Khan, Y. Peng, E. Steinbach, M. Sgroi, and W. Kellerer, "Application-driven cross-layer optimization for video streaming over wireless networks," *IEEE Commun. Mag.*, vol. 44, no. 1, pp. 122–130, Jan. 2006.
- [36] Y. Huh, M. Hu, M. Reisslein, and J. Zhang, "MAI-JSQ: A cross-layer design for real-time video streaming in wireless networks," Telecommun. Res. Center, Dept. Elect. Eng., Arizona State Univ., Tempe, AZ, USA, Aug. 2002.
- [37] L.-U. Choi, W. Kellerer, and E. Steinbach, "Cross layer optimization for wireless multi-user video streaming," in *Proc. Int. Conf. Image Process. (ICIP)*, Oct. 2004, pp. 2047–2050.
- [38] M. Ivrlac and J. Nassek, "Cross layer design—An equivalence class approach," *IEEE Commun. Mag.*, vol. 43, no. 12, pp. 112–119, Dec. 2005.
- [39] P. Chou and Z. Miao, "Rate-distortion optimized streaming of packetized media," Microsoft Research, Redmond, WA, USA, Tech. Rep. MSR-TR-2001-35, Feb. 2001.
- [40] M. van der Schaar and M. Tekalp, "Integrated multi-objective cross-layer optimization for wireless multimedia transmission," in *Proc. IEEE Int. Symp. Circuits Syst.*, May 2005, pp. 3543–3546.
- [41] D. Wu, S. Ci, and H. Wang, "Cross-layer optimization for video summary transmission over wireless networks," *IEEE J. Sel. Areas Commun.*, vol. 25, no. 4, pp. 841–850, May 2007.
- [42] V. G. Gudise and G. K. Venayagamoorthy, "Comparison of particle swarm optimization and back propagation as training algorithms for neural networks," in *Proc. IEEE Swarm Intell. Symp. (SIS)*, Apr. 2003, pp. 110–117.
- [43] J. Robinson and Y. Rahmat-Samii, "Particle swarm optimization in electromagnetics," *IEEE Trans. Antennas Propag.*, vol. 52, no. 2, pp. 397–407, Feb. 2004.
- [44] Z. Chen, M. Li, and Y.-P. Tan, "Perception-aware multiple scalable video streaming over WLANs," *IEEE Signal Process. Lett.*, vol. 17, no. 7, pp. 675–678, Jul. 2010.
- [45] A. Abdel Khalek, C. Caramanis, and R. W. Heath, "A cross-layer design for perceptual optimization of H.264/SVC with unequal error protection," *IEEE J. Sel. Areas Commun.*, vol. 30, no. 7, pp. 1157–1171, Aug. 2012.
- [46] Z. Yang and X. Wang, "Scalable video broadcast over downlink MIMO-OFDM systems," *IEEE Trans. Circuits Syst. Video Technol.*, vol. 23, no. 2, pp. 212–223, Feb. 2013.
- [47] X. Du, N.-S. Vo, W. Cheng, T. Q. Duong, and L. Shu, "Joint replication density and rate allocation optimization for VoD systems over wireless mesh networks," *IEEE Trans. Circuits Syst. Video Technol.*, vol. 23, no. 7, pp. 1260–1273, Jul. 2013.
- [48] S.-M. Tseng and Y.-F. Chen, "Average PSNR optimized cross layer user grouping and resource allocation for uplink MU-MIMO OFDMA video communications," *IEEE Access*, vol. 6, pp. 50559–50571, 2018.
- [49] C. Li, D. Wu, and H. Xiong, "Delay—Power-rate-distortion model for wireless video communication under delay and energy constraints," *IEEE Trans. Circuits Syst. Video Technol.*, vol. 24, no. 7, pp. 1170–1183, Jul. 2014.
- [50] X. Chen, J.-N. Hwang, C.-N. Lee, and S.-I. Chen, "A near optimal QoE-driven power allocation scheme for scalable video transmissions over MIMO systems," *IEEE J. Sel. Topics Signal Process.*, vol. 9, no. 1, pp. 76–88, Feb. 2015.
- [51] M. I. Salman, M. Q. Abdulhasan, C. K. Ng, N. K. Noordin, B. M. Ali, and A. Sali, "A partial feedback reporting scheme for LTE mobile video transmission with QoS provisioning," *Comput. Netw.*, vol. 112, pp. 108–121, Jan. 2017.
- [52] H. Karim, N. S. Anil Shah, N. M. Arif, A. Sali, and S. Worrall, "Reduced resolution depth coding for stereoscopic 3D video," *IEEE Trans. Consum. Electron.*, vol. 56, no. 3, pp. 1705–1712, Aug. 2010.
- [53] Q. Lin, S. Liu, Q. Zhu, C. Tang, R. Song, J. Chen, C. A. C. Coelho, K.-C. Wong, and J. Zhang, "Particle swarm optimization with a balanceable fitness estimation for many-objective optimization problems," *IEEE Trans. Evol. Comput.*, vol. 22, no. 1, pp. 32–46, Feb. 2018.
- [54] P. Zhao, Y. Liu, J. Liu, S. Ci, and R. Yao, "SSIM-based error-resilient rate-distortion optimization of H.264/AVC video coding for wireless streaming," *Signal Process., Image Commun.*, vol. 29, no. 3, pp. 303–315, Mar. 2014.
- [55] D. Wang, Y. Peng, X. Ma, W. Ding, H. Jiang, F. Chen, and J. Liu, "Adaptive wireless video streaming based on edge computing: Opportunities and approaches," *IEEE Trans. Services Comput.*, vol. 12, no. 5, pp. 685–697, Sep. 2019.



YAKUBU S. BAGUDA (Senior Member, IEEE) was born in Kano, Nigeria. He received the B.Eng. degree in electrical engineering from Bayero University, Nigeria, in 2001, the M.Sc. degree in information systems from Robert Gordon University, Aberdeen, U.K., in 2003, and the Ph.D. degree (Hons.) in electrical engineering from the University of Technology, Malaysia, in 2010.

From 2011 to 2012, he was a Postdoctoral Researcher with the UTM-MIMOS Centre of Telecommunication Excellence, Malaysia. He is currently an Assistant Professor with the Faculty of Computing and Information Technology, King Abdulaziz University, Saudi Arabia. He is the author of more than 30 journal articles and conference papers. His research interests include game theory, e-healthcare systems, cross layer design and optimization, energy-efficient schemes, system modeling and prediction, intelligent decision systems, cognitive radio systems, resource allocation and management, network optimization and performance analysis, bio inspired optimization algorithms, and wireless multimedia communication and networking.

Dr. Baguda is a Senior Member of ACM. He received the Chartered Engineer (C.Eng.) Award from the U.K. Engineering Council, in 2017.

• • •